

# Quantitative Analysis of Neanderthal Temporal Bone Morphology Using Three-Dimensional Geometric Morphometrics

Katerina Harvati\*

*Department of Anthropology, New York University, New York, New York 10003*

**KEY WORDS** Neanderthals; modern human origins; human variation; temporal bone

**ABSTRACT** The temporal bone is the location of several traits thought to differentiate Neanderthals from modern humans, including some proposed Neanderthal-derived traits. Most of these, however, are difficult to measure and are usually described qualitatively. This study applied the techniques of geometric morphometrics to the complex morphology of the temporal bone, in order to quantify the differences observed between Neanderthal and modern human anatomy. Two hundred and seventy modern human crania were measured, representing 9 populations of 30 individuals each, and spanning the extremes of the modern human geographical range. Twelve Neanderthal specimens, as well as Reilingen, Kabwe, Skhul 5, Qafzeh 9, and 4 Late Paleolithic European specimens, were included in the fossil sample. The data were collected in the form of three-dimensional (3-D) landmark

coordinates, and specimen configurations were superimposed using generalized Procrustes analysis. The fitted coordinates were then analyzed by an array of multivariate statistical methods, including principal components analysis, canonical variates analysis, and Mahalanobis  $D^2$ . The temporal bone landmark analysis was very successful in separating Neanderthals from modern humans. Neanderthals were separated from modern humans in both the principal components and canonical variates analyses. They were much further in Mahalanobis distances from all modern human populations than any two modern human groups were from each other. Most of the previously described temporal bone traits contributed to this separation. *Am J Phys Anthropol* 120:323–338, 2003. © 2003 Wiley-Liss, Inc.

The temporal bone is one of the most diagnostic anatomical areas for Neanderthals, as it is the location of several traits thought to differentiate this fossil human group from modern humans (Trinkaus and Smith, 1985; Vandermeersch, 1985; Condemi, 1991; Elyaqtime, 1996). These traits include the small size of the mastoid process relative to the large juxtamastoid eminence, a proposed derived feature (Boule and Vallois, 1957; Vallois, 1969; Santa Luca, 1978; Stringer et al., 1984; Stringer, 1985; Hublin, 1988a; Condemi, 1991, 1992; Arsuaga et al., 1993; Elyaqtime, 1996; Dean et al., 1998; Minugh-Purvis et al., 2000); the supero-inferiorly low and antero-posteriorly short squama (Boule and Vallois, 1957; Vallois, 1969; Heim, 1976); the origin of the petrotympanic crest at the most inferiorly projecting part of the tympanic and the coronal orientation of the tympanic plate (Vallois, 1969; Trinkaus, 1983; Vandermeersch, 1985; Condemi, 1992; Elyaqtime, 1996; Schwartz and Tattersall, 1996a; Minugh-Purvis et al., 2000); the elevated position of the external auditory meatus relative to the zygomatic process and the floor of the glenoid fossa (Vallois, 1969; Stringer et al., 1984; Vandermeersch, 1985; Elyaqtime, 1995b); a wide, shallow, and medially closed-off glenoid fossa (Vallois, 1969); the robusticity and lateral projection of the zygomatic process and the strong

supramastoid crest (Boule and Vallois, 1957; Vallois, 1969; Heim, 1976); and an anteriorly closed off digastric fossa (Vallois, 1969; Vandermeersch, 1985; Martínez and Arsuaga, 1997; Minugh-Purvis et al., 2000). Most of these characteristics are difficult to measure directly with traditional caliper measurements, and as a consequence have not been subject to rigorous quantitative analysis.

The purpose of this study was to quantitatively evaluate the presence and degree of expression of these temporal bone traits in modern human populations and in Neanderthal specimens. Their quantification was made possible with the use of three-dimensional (3-D) geometric morphometrics, which

Grant sponsor: NSF Dissertation Improvement and NYCEP RTG; Grant sponsor: American Museum of Natural History; Grant sponsor: Onassis Foundation; Grant sponsor: CARE Foundation.

\*Correspondence to: Katerina Harvati, Department of Anthropology, New York University, 25 Waverly Place, New York, NY 10003. E-mail: katerina.harvati@nyu.edu

Received 11 January, 2002; accepted 3 April, 2002.

DOI 10.1002/ajpa.10122  
Published online in Wiley InterScience (www.interscience.wiley.com).

TABLE 1. List of specimens by population and sex for comparative modern human sample<sup>1</sup>

Group	Male	Female	Undetermined	Total
Modern humans	143	126	1	270
Andamanese (Andaman Islands, India, BMNH)	13	17		30
Australians (New S. Wales, S. Australia, BMNH)	19	11		30
Berg (Austria, AMNH)	15	15		30
Dogon (Mali, West Africa, MH)	15	15		30
Epipaleolithic (Afalou, Taforalt, IPH)	18	12		30
Inugsuk (Greenland, UC)	15	15		30
West Eurasian (Egypt, Dalmatia, Greece, Italy, Germany, AMNH)	17	12	1	30
Khoisan (South Africa, UV)	16	14		30
Tolai (New Britain, Melanesia, AMNH)	15	15		30

<sup>1</sup> AMNH, American Museum of Natural History, New York; BMNH, British Museum (Natural History), London; IPH, Institut de Paléontologie Humaine, Paris; MH, Musée de l'Homme, Paris; UC; University of Copenhagen; UV, University of Vienna; S, South.

were applied to the complex detailed morphology of the temporal bone. Geometric morphometrics is advantageous relative to traditional morphometrics in that it better preserves the geometry of the object studied, and it allows visualization of shape differences between specimens and between group means in specimen shape (Rohlf and Marcus, 1993; O'Higgins and Jones, 1998). Perhaps the greatest advantage of this technique, however, is that it provides a means of quantifying shape differences, and therefore differences in character states, of variable traits which cannot be directly linearly measured (Dean, 1993; Harvati, 2001a).

## MATERIALS AND METHODS

This study included a comparative sample of nine modern human populations and a fossil sample comprising several Middle and Late Pleistocene hominid specimens. The comparative modern human sample included nine modern human populations, each consisting of approximately 30 individuals, comprising a total of 270 specimens (Table 1). Following the seminal study of Howells (1973, 1989), each modern human population was chosen to represent a biological population limited in space and time. When possible, subsamples of the populations of Howells (1973, 1989) were used. The Epipaleolithic samples from Afalou and Taforalt, dated to 14–8.5 ka (Lahr, 1996), were merged to represent one population, which was included in order to give a time dimension in the comparative sample. A mixed Eurasian population, represented by samples of six individuals each from four localities across Western Eurasia, was also measured. Only adult crania were measured, as determined by a fully erupted adult dentition. Sex was unknown in most cases, and was assessed by inspection during study and following the sexing assessments of Howells (1973, 1989). When possible, equal numbers of male and female specimens were measured.

The fossil human sample included 12 Neanderthal specimens from Europe and the Near East; the early Neanderthal specimen from Reilingen; the Middle Pleistocene African specimen Kabwe; two early anatomically modern humans from the Near East; and four Late Paleolithic anatomically modern humans

from Europe (Table 2). Where the original fossils were unavailable, high-quality casts from the Anthropology Department of the American Museum of Natural History were measured. Sex was assigned, using a variety of sources from the literature (McCown and Keith, 1937; Genoves, 1954; Boule and Vallois, 1957; Jelinek, 1969; Oakley et al., 1971; Smith, 1980; Vandermeersch, 1981; Radovic et al., 1988; Delson et al., 2001). As most fossil specimens were incomplete, analysis was undertaken in two steps, varying in number of landmarks and in the fossil sample included, so as to maximize the number of specimens and landmarks used. The first step of analysis (referred from here onwards as step 1) included six Neanderthal specimens and 15 landmarks. The removal of the two landmarks on the zygomatic arch allowed for the inclusion of 12 Neanderthal specimens in the second step of analysis (referred to as step 2). The landmarks and specimens used in each of the two steps are listed in Tables 2 and 3.

Fifteen temporal landmarks were digitized, most representing standard osteological landmarks, following the definitions given in Howells (1973). Other landmarks were also included, and their definitions are given in Table 3. Figure 1 shows the temporal bone landmarks in lateral and ventral view on a modern human cranium. All 15 landmarks were included in step 1, while step 2 only included 13 landmarks.

The data were collected in the form of 3-D coordinates of the 15 temporal bone landmarks, using the portable digitizer Microscribe 3DX. Minimal reconstruction was allowed during data collection for specimens where very little damage in a particular area of interest was observed. The landmark coordinate data were processed using generalized Procrustes analysis, which superimposes the landmark configurations of the specimens and scales them for size, so that the differences they exhibit are due to "shape" (Rohlf, 1990; Rohlf and Marcus, 1993; Slice, 1996; O'Higgins and Jones, 1998). The Procrustes methods have been shown to have the highest statistical power among alternative geometric morphometric approaches (Rohlf, 2000). Superimposition was performed using the software GRF-ND and

TABLE 2. List of fossil human specimens measured<sup>1</sup>

NDR	EAM	LP	MPL
<b>Male</b>			
Saccopastore 2 (1–2, ULS)	Skhul 5 (1–2*)	Cro Magnon 1 (1–2*)	Kabwe (1–2, BMNH)
La Chapelle (1–2*)		Predmosti 3 (1–2*)	
La Ferrassie 1 (1–2*)			
Shanidar 1 (1–2*)			
Circeo 1 (1–2, MP)			
Amud 1 (1–2, UTA)			
Spy 2 (2, IRSN)			
<b>Female</b>			
Gibraltar 1 (2, BMNH)	Qafzeh 9 (2, UTA)	Predmosti 4 (2*)	
Krapina C (2, CMNH)		Mladec 2 (2, NHM)	
Krapina 39-1 (2, CMNH)			
Spy 1 (2, IRSN)			
<b>Sex unknown</b>			
La Quina 27 (2, IPH)			Reilingen (2, SMN)

<sup>1</sup> Steps of analysis in which each specimen was included and the institution where the specimen is curated are indicated in parentheses. Asterisks indicate specimens for which casts from the AMNH were measured. NDR, Neanderthal; EAM, early anatomically modern; LP, Late Paleolithic; MPL, Middle Paleolithic specimens. CNHM, Croatian Natural History Museum, Zagreb; IRSN, Institut Royal des Sciences Naturelles, Brussels; NHM, Naturhistorisches Museum, Vienna; SMN Staatliches Museum für Naturkunde, Stuttgart; ULS, Università La Sapienza, Rome; UTA, University of Tel Aviv. Other institutional abbreviations as in Table 1.

TABLE 3. Landmarks collected on temporal and occipital bones, as well as along posterior cranial profile<sup>1</sup>

Temporal bone landmarks	
1. Asterion	(Steps 1–2)
2. Stylomastoid foramen	(Steps 1–2)
3. Most medial point of jugular fossa	(Steps 1–2)
4. Most lateral point of jugular fossa	(Steps 1–2)
5. Lateral origin of petrotympanic crest	(Steps 1–2)
6. Most medial point of petrotympanic crest at level of carotid canal	(Steps 1–2)
7. Porion	(Steps 1–2)
8. Auriculare	(Steps 1–2)
9. Parietal notch	(Steps 1–2)
10. Mastoidiale	(Steps 1–2)
11. Most inferior point on juxtamastoid crest (following Hublin, 1978a)	(Steps 1–2)
12. Deepest point of lateral margin of articular eminence (root of articular eminence)	(Steps 1–2)
13. Suture between temporal and zygomatic bones on inferior aspect of zygomatic process	(Step 1)
14. Suture between temporal and zygomatic bones on superior aspect of zygomatic process	(Step 1)
15. Most inferior point on entoglenoid process	(Steps 1–2)

<sup>1</sup> In parentheses are levels of analysis in which each landmark was used.

Morpheus (Slice, 1992, 1994–1999). The specimen configurations were translated to a common origin, scaled to unit centroid size (the square root of the sum of squared distances of all landmarks to the centroid of the object, i.e., the measure of size used here), and rotated according to a best-fit criterion. Figure 2 shows the superimposed mean Neanderthal and modern human configurations.

Since reflection of right and left side is possible in GRF-ND, it was possible to combine in one sample fossil specimens preserving the temporal bone on different sides. As the majority of fossil specimens still exhibited many missing landmarks, data were reconstructed by mirror imaging for right-left ho-

mologous landmarks. In this way, landmarks preserved on different sides could be combined to form a more complete composite temporal bone landmark configuration for an incompletely preserved specimen.

The fitted coordinate configurations resulting from Procrustes superimposition were thought to lie in Kendall's shape space (Rohlf, 1996). However, Slice (2001) found that they lie in a hemispherical variant of this shape space. As in both cases, shape space is non-Euclidean, a projection of these coordinates to tangent space is usually recommended for statistical analysis. However, biological data are restricted in their variation, and the shape space coordinates are almost identical to their projections in tangent space (Slice, 2001). This assumption was tested in the temporal bone landmark dataset, using TPSSMALL (Rohlf, 1998), which compares Procrustes distances to Euclidean distances. The correlation between the two distances was found to be very strong (correlation 0.9998, and root MS error 0.0004), and the statistical analysis was performed on the fitted coordinates themselves.

The coordinates were analyzed using principal components analysis, canonical variates analysis, and Mahalanobis  $D^2$  analysis. Visualization of results was performed in GRF-ND and Morpheus. Centroid size was analyzed first, in order to assess differences in size among Neanderthals, the other fossil specimens included, and modern human populations. An analysis of variance (ANOVA) was conducted on centroid size to determine whether there were significant differences in centroid size between groups and between males and females. The fitted coordinate configurations of the specimens were analyzed using principal components analysis (PCA), in order to explore how variation is partitioned within and among the samples, as well as to achieve

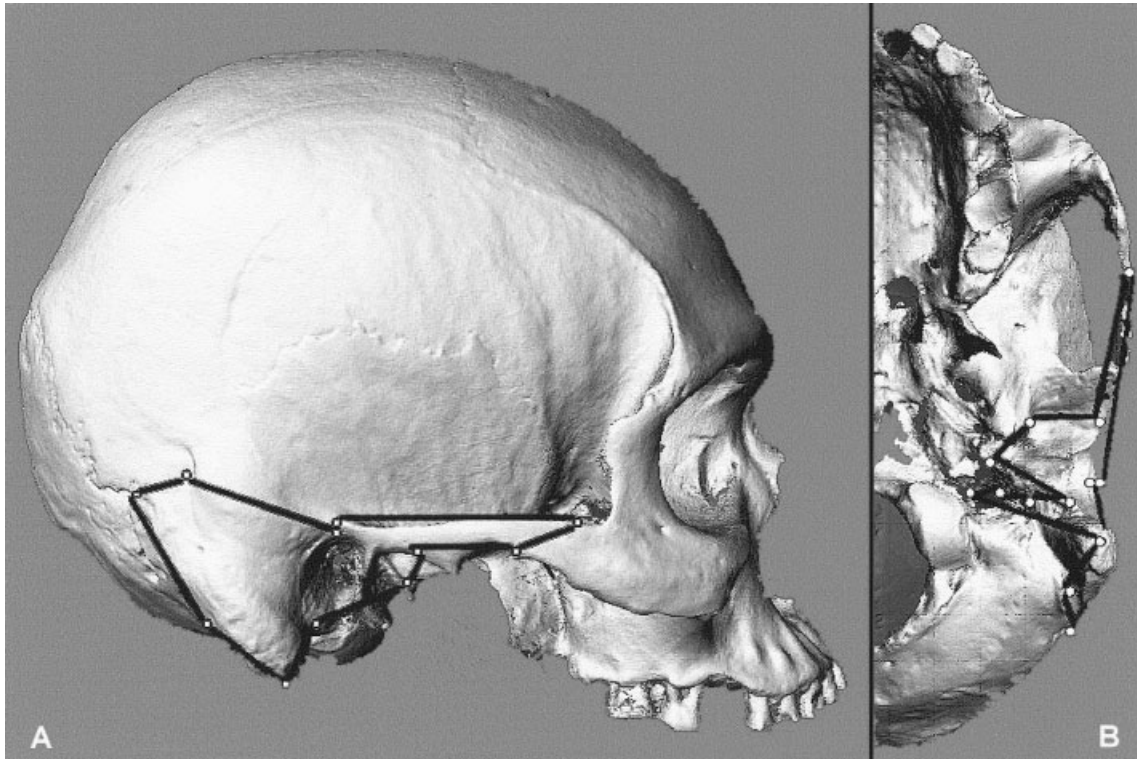


**Fig. 1.** Temporal bone landmarks, shown on a modern human skull. Dots represent landmarks; black lines between landmarks are links used for convenience in visualization. **A:** Lateral view. **B:** Ventral view.

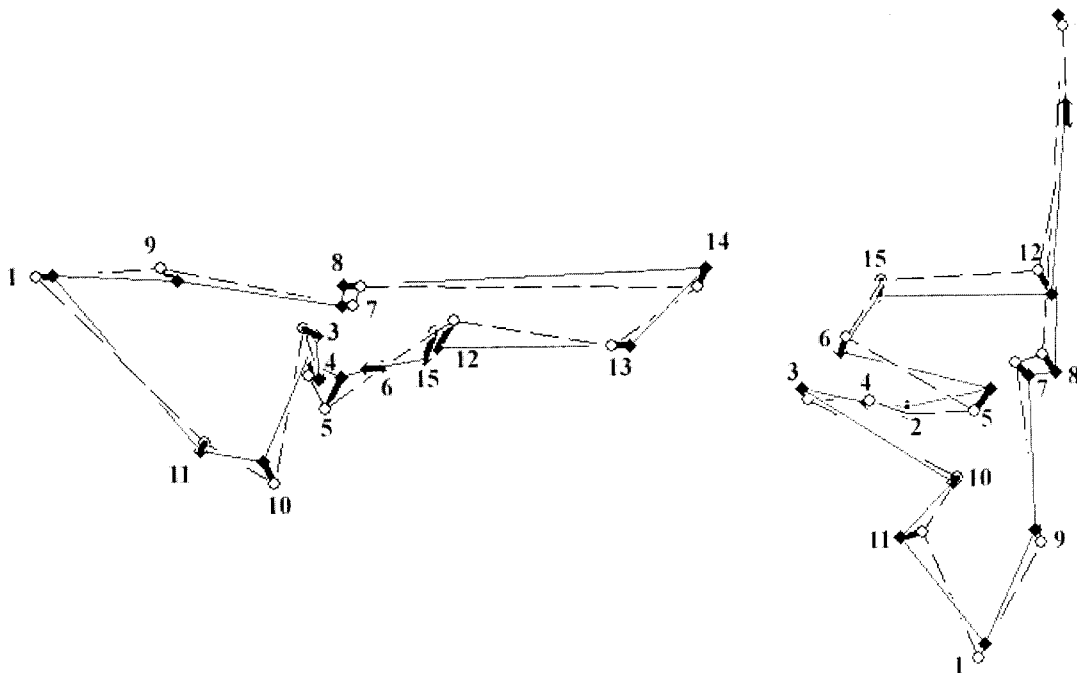


**Fig. 2.** Superimposed mean temporal landmark configurations for Neanderthals and modern humans. Solid diamonds, Neanderthals; open circles, modern humans. Lines between landmarks are links used for convenience in visualization. Solid, Neanderthals; dashed, modern humans. Bold lines show shape differences at each landmark. Landmarks are described in Table 3; landmark numbers correspond to those given there.

data reduction. An ANOVA was performed on the PCA scores to determine the significance of population, sex, and interaction effects along each compo-

nent. Furthermore, a Bonferroni test (alpha set to 0.05) was performed on all pairwise comparisons of the population and sex means of the principal com-

TABLE 4. Unbiased Mahalanobis  $D^2$  matrices, step 1 (above) and step 2 (below)<sup>1</sup>

	And	Aus	Brg	Dgn	Epi	Igs	Eur	Kbw	San	Skh5	Tol	LP	Nea
And	0.00												
Aus	24.34	0.00											
Brg	29.32	16.70	0.00										
Dgn	26.23	21.56	27.88	0.00									
Epi	35.30	24.73	18.35	23.88	0.00								
Igs	31.53	13.44	25.13	18.29	26.61	0.00							
Eur	26.99	11.67	4.64	17.69	14.90	17.41	0.00						
Kbw	59.38	51.57**	58.17**	58.45**	60.23	72.52	57.54**	0.00					
San	40.68	23.62	30.72	14.57	32.66	28.05	25.32	53.15**	0.00				
Skh5	113.59	93.91	93.30	124.93	108.36	118.37	98.69	140.73	130.55	0.00			
Tol	25.90	6.98	17.14	23.47	24.97	13.51	11.73	68.83	25.76	108.87	0.00		
LP	73.45	53.79	38.88	71.68	41.96	39.22	43.88	97.98	66.86	89.03	47.59	0.00	
Nea	94.34	74.45	87.72	73.18	73.10	62.65	80.18	76.84	83.59	149.93	84.71	92.35	0.00

	And	Aus	Brg	Dgn	EAM	Epi	Igs	Eur	Kbw	Rei	San	Tol	LP	Nea
And	0.00													
Aus	28.22	0.00												
Brg	22.33	14.34	0.00											
Dgn	23.26	18.46	17.65	0.00										
EAM	71.29	95.32	76.48	96.98	0.00									
Epi	34.28	28.58	15.82	19.53	92.89	0.00								
Igs	31.43	14.16	21.15	17.55	100.78	27.89	0.00							
Eur	20.93	9.86	4.38	10.42	84.87	13.15	15.00	0.00						
Kbw	41.06*	28.83 (NS)	39.50*	36.50*	116.06	34.95(NS)	39.99*	36.40*	0.00					
Rei	172.97	135.77	131.86	124.12	211.18	101.39	111.42	126.89	125.37	0.00				
San	38.04	22.43	24.92	15.05	116.28	33.69	31.38	23.14	31.89 (NS)	142.18	0.00			
Tol	24.24	6.56	11.48	15.96	94.66	24.16	14.31	7.31	37.87*	145.88	20.82	0.00		
LP	33.13	27.66	17.53	32.11	84.36	20.41	18.87	20.48	25.41 (NS)	117.77	39.16	24.77	0.00	
Nea	79.57	63.02	73.07	64.85	103.90	60.08	49.74	69.74	44.66*	80.41	75.83	75.73	63.11	0.0

<sup>1</sup> All distances reported are significant at 0.001 level, except NS, nonsignificant; \* 0.05 level; \*\* 0.01 level. And, Andamanese; Aus, Australian; Brg, Berg; Dgn, Dogon; Epi, Epipaleolithic; Igs, Inugsuk; Eur, mixed European; Kbw, Kabwe; San, Khoisan; Skh5, Skhul 5; EAM, early anatomically modern humans; Tol, Tolai; LP, Late Paleolithic; Nea, Neanderthal.

ponent and canonical variates scores, in order to detect significant differences between groups. This is a conservative test, and significant differences found at the preset level of alpha have a somewhat greater level of significance.

The shape differences along the components separating Neanderthals, or other fossils, from modern humans were explored. The influence of each landmark was assessed by inspection of the eigenvector coefficients of each variable for that component, and by visualizing the shape variation at each landmark along each principal component (PC) in GRF-ND. This was achieved by plotting the eigenvector coefficients for each PC on the consensus configurations, allowing for visualization of a hypothetical configuration at the extremes of each PC (Slice, 1996). A correlation analysis with centroid size was performed for the scores of each PC, in order to determine the significance of centroid size variation in the variation along that component and to identify allometric effects.

A canonical variates analysis (CVA) was conducted on the principal component scores, in order to maximize the separation between groups and to evaluate the shape differences that best separate them. The first 30 principal components were used, accounting for 97% and 99.4% of the total variance, respectively, for steps 1 and 2. Unlike PCA, this analysis uses group membership information. The group information used here was population membership rather than species information, so as not to bias the results toward separation of pre-designated species. In order to visualize shape differences along

each canonical axis in shape space, the canonical scores for each axis were regressed on the fitted coordinates. The regression coefficients obtained were inputted in GRF-ND and plotted on the fitted configurations in the same way as the principal components eigenvector coefficients (see above). This procedure allowed for visualization of the shape differences at each landmark along each canonical axis (Marcus, personal communication). As with the principal components, a correlation analysis with centroid size was performed, in order to determine how much of the variation along that canonical variate can be explained by variation in centroid size. Finally, Mahalanobis  $D^2$  matrices were calculated for the groups included in the analysis and for each step of the analysis, correcting for unequal sample sizes (Marcus, 1993). They are reported in Table 4.

## RESULTS

### Centroid size

Neanderthals fell within the range of the modern human centroid size for the temporal bone, and were not significantly different from most modern human populations in this measure. Centroid size differences were also relatively small between males and females, although there was a significant overall sex effect. The female mean was significantly lower than the male mean, and females showed a smaller standard deviation than males.

### Principal components analysis

**Step 1.** In the first step of analysis, Neanderthals were separated from modern humans along PC 9

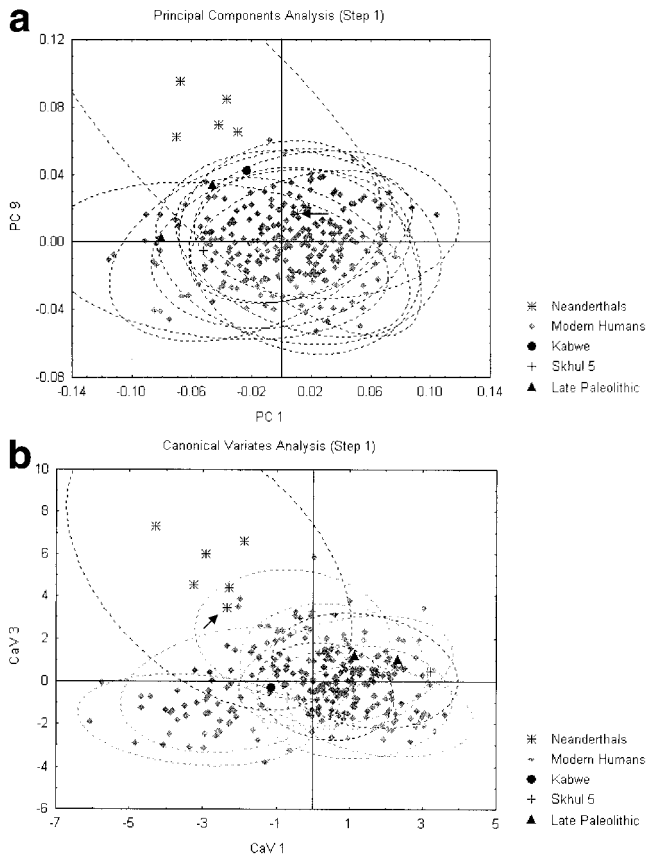


**Fig. 3.** **a:** Principal components analysis (step 1), PCs 1 and 9. Dotted lines represent 95% confidence ellipses for each population. Arrow indicates position of Amud 1. **b:** Canonical variates analysis (step 1), CVAs 1 and 3. Dotted lines represent 95% confidence ellipses for each population. Arrow indicates position of Amud 1.

(Fig. 3a). This component explained 4.05% of the total variance (PCs 1–9 explain 67% of the total variance), and was not correlated with centroid size. Neanderthals were significantly different in their mean score for this component from all modern human populations. Amud 1 was the only Neanderthal specimen which fell within the modern human range, along PC 9. The shape differences along this component included a more laterally placed porion, auriculare, and mastoid process, a more anteriorly placed lateral end of the petrotympanic crest, a more inferiorly placed root of the articular eminence (measured at the lateral margin of the glenoid fossa), and a more posterior and somewhat lateral position of the entoglenoid process in Neanderthals relative to modern humans.

Significant sex ( $P = 0.01$ ) effects were found for PC 1 (12.2% of the total variance; Fig. 3a). The overall female mean score was significantly more negative than the male score. Furthermore, in all modern human populations, the female mean score were more negative than the male mean score of the same population, indicating a consistent pattern of sexual dimorphism across all modern human groups. No population effect was observed, although

some of the Khoisan individuals were found to have extremely negative scores. The shape differences characterizing modern human females relative to males included a small mastoid process and juxtamastoid eminence, an antero-posteriorly long and supero-inferiorly short mastoid portion of the temporal bone, and an antero-posteriorly elongated zygomatic process. Although all Neanderthal specimens included in this sample are considered male, their scores along this principal component were negative, with the exception of Amud 1. PC 1 was not correlated with centroid size.

Kabwe was separated from both the modern human and the Neanderthal sample along PC 3 (8.8% of the total variance, not correlated with centroid size). The shape differences that characterized this specimen included a more inferiorly placed asterion, a more posteriorly placed juxtamastoid eminence, and an inferiorly placed zygomatic suture.

Principal components 2 and 4–7 involved differences between modern human populations, although no clear separation between populations was observed. The strongest population effect was seen in PC 2 (11.1% of total variance, not correlated with centroid size), which separated the Andamanese from the other modern human populations, although there was substantial overlap among modern human groups. The Andamanese were significantly different in their mean scores from the Tolai, the Khoisan, the Berg, and the Late Paleolithic population, but not from other modern human groups. The shape differences that tend to characterize the Andamanese relative to other modern humans included a more anterior position of the parietal notch, indicating a longer mastoid portion of the temporal bone, and a more posterior and slightly superior position of the tip of the juxtamastoid eminence.

PC 8 (4.2% of total variance, not correlated with centroid size) separated the two Late Paleolithic specimens, as well as Skhul 5, from modern humans and Neanderthals. The Late Paleolithic specimens were significantly different from all other human populations in their mean scores for this component. The shape differences that characterized these specimens relative to other modern humans and Neanderthals included an inferior position of the parietal notch and a superior position of asterion, as well as a more posterior placement of the anterior margin of the jugular fossa and a superior placement of the medial end of the petrotympanic crest.

Skhul 5 falls at the extreme of the modern human range of variation along PC 12 (2.7% of total variance), indicating a more postero-superiorly to antero-inferiorly inclined temporo-zygomatic suture and a more superiorly and medially placed lateral end of the petrotympanic crest relative to most modern humans. PCs 10–11 and 13–16 did not show any clear separation or significant differences among modern human groups or the fossil samples included here. Components 1–16 explain 81.2% of the total

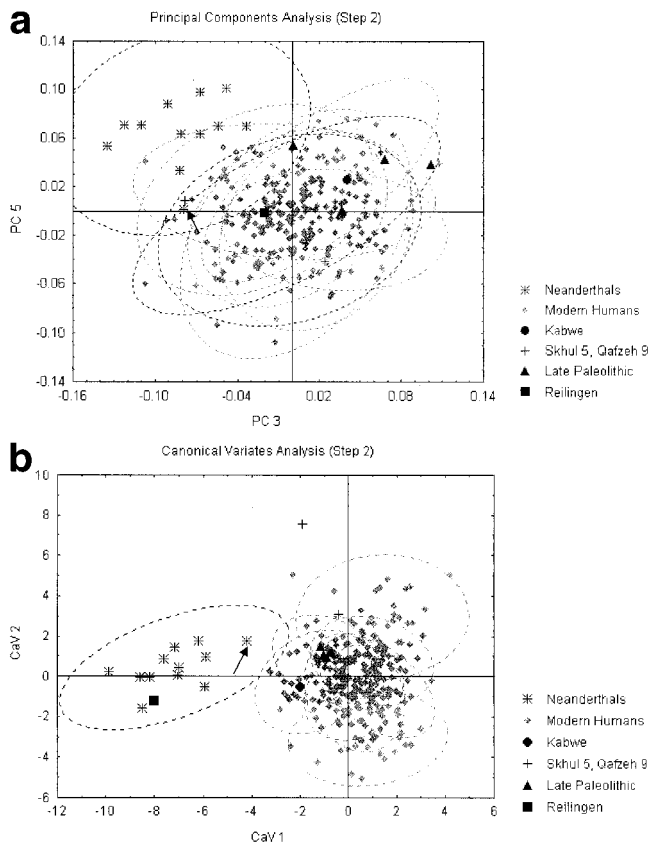


**Fig. 4.** **a:** Principal components analysis (step 2), PCs 3 and 5. Dotted lines represent 95% confidence ellipses for each population. Arrow indicates position of Amud 1. **b:** Canonical variates analysis (step 2), CVAs 1 and 2. Dotted lines represent 95% confidence ellipses for each population. Arrow indicates position of Amud 1.

variance. Higher components explain less than 2% of the total variance each.

**Step 2.** In the second step of the analysis, Neanderthals were significantly different from most modern human populations along PC 5 (6.3% of total variance; Fig. 4a). The shape differences along PC 5 included a more anterior placement of the lateral origin of the petrotympanic crest, a more anterior placement of asterion, a more anterior and superior position of the tip of the mastoid process, and a more inferior placement of the juxtamastoid eminence. Neanderthals are also partially separated along PC 3 (8.7% of total variance; Fig. 4a). Along both of these principal components, Qafzeh 9 falls in the area of overlap between Neanderthals and modern humans and very close to Amud 1. The shape differences along this component included a more medial placement of the juxtamastoid eminence, a more posterior parietal notch, and a more laterally placed auriculare in Neanderthals relative to modern humans. Neither PC 3 nor 5 was correlated with centroid size.

Kabwe was separated from modern humans along PC 1 (13.2% of total variance, not correlated with

centroid size). The shape differences that characterized this specimen included a more inferiorly placed asterion, an inferiorly placed parietal notch, a posteriorly placed juxtamastoid eminence, and a superiorly placed tip of the mastoid process. As in step 1, significant sex effects were also found for this component. The overall male mean score was significantly more positive than the female mean score. However, unlike in step 1, the mean male scores for each population tended to be more positive than the females across most, but not all, groups. Among recent human populations, the West African Dogon showed the opposite pattern, while the Austrian Berg and the Andamanese showed almost identical means for the two sexes. Although sex assignment in fossil specimens is problematic, the Neanderthal female mean score was also more positive than the male score, following the pattern shown by the majority of modern human groups. The Late Paleolithic specimens, however, as well as Skhul 5 and Qafzeh 9, showed the opposite pattern. The shape differences that tended to characterize females relative to males in most modern human populations and in Neanderthals included a small mastoid process and an antero-posteriorly elongated and supero-inferiorly short mastoid portion of the temporal bone. These shape differences are similar to those found between the two sexes in step 1. The stronger effect of sexual dimorphism in step 1 may be related to the inclusion of the two zygomatic suture landmarks, which contributed to the separation between males and females.

PCs 2 and 4 reflected differences between modern human populations, although no clear separation between populations was observed. The Andamanese and Epipaleolithic populations fell on one end of the human range along PC 2 (11% of total variance, not correlated with centroid size), while the Eskimo and the Khoisan fell on the opposite end. However, there is substantial overlap, and none of these populations are significantly different from the others in their mean scores. The separation is even less clear along PC 4 (7.5% of total variance, not correlated with centroid size). Reilingen falls outside the modern human range along this component, overlapping, however, with the extreme of the Neanderthal range. The shape differences that characterize this specimen relative to modern humans and most Neanderthals include a more posteriorly placed asterion and anteriorly placed parietal notch, reflecting a long mastoid portion of the temporal bone, and an anterior position of the mastoidale.

PCs 6–15 do not show any separation or significant differences among the modern human populations or the fossil groups and specimens included here. The first 15 components explain 83.3% of the total variance, while higher components explain very small percentages of the total variance each (<2%).

### Canonical variates analysis

**Step 1.** Neanderthals were separated from modern humans on the positive extreme of CVA 3 in step 1 (Fig. 3b). CVA 1 and 2 separated groups of modern human populations from each other. Along CVA 1 (22.06% of total variance, not correlated with centroid size; Fig. 3b), the two African populations were separated from other modern human groups, although there was some overlap of the West African Dogon with the Inugsuk Eskimo population. Neanderthals and Kabwe also overlapped with the African populations. The Khoisan population was significantly different along this canonical axis from all other groups except the West African Dogon and the Neanderthals. The shape differences that tended to characterize the Khoisan, and to a lesser extent the Dogon and Neanderthals, included a smaller mastoid process, a more medially placed tip of the juxtamastoid eminence, and a more superior placement of the medial end of the petrotympanic crest. The second canonical axis (18.81% of total variance, not strongly correlated with centroid size) separated the Andamanese from the other human groups. This population was significantly different in its mean scores from all other populations. Neanderthals and the two Late Paleolithic specimens both fell at the opposite end of the human range from the Andamanese. Both were significantly different from the Andamanese, but not from the other modern human groups. The shape differences that characterized the Andamanese population relative to other modern humans included an anterior placement of the parietal notch, a more superior and posterior placement of the root of the articular eminence, a more anterior position of the entoglenoid process, and a more superior placement of the temporo-zygomatic suture. The opposite shape differences tended to characterize Neanderthals and the Late Paleolithic group, although these differences did not separate them from modern humans.

CVA 3 (Fig. 3b) explained 16% of the total variance, was mostly influenced by PC 3, and was not correlated with centroid size. Neanderthals were significantly different from all modern human populations in their mean score. However, Amud 1 again fell within the 95% confidence ellipses of some modern human populations. The shape differences along this canonical axis, as visualized in GRF-ND, included an elevated position of the superior aspect of the zygomatic suture, a more superior and lateral placement of the auriculare, an inferior placement of the root of the articular eminence and the tip of the entoglenoid process, an anterior lateral origin and posterior medial end of the petrotympanic crest, an elevated and anteriorly placed asterion, and a superior placement of the tip of the mastoid process (Fig. 5).

**Step 2.** In step 2, Neanderthals were separated from modern humans along the first canonical axis (Fig. 4b). CVA 1 explained 25.4% of the total vari-

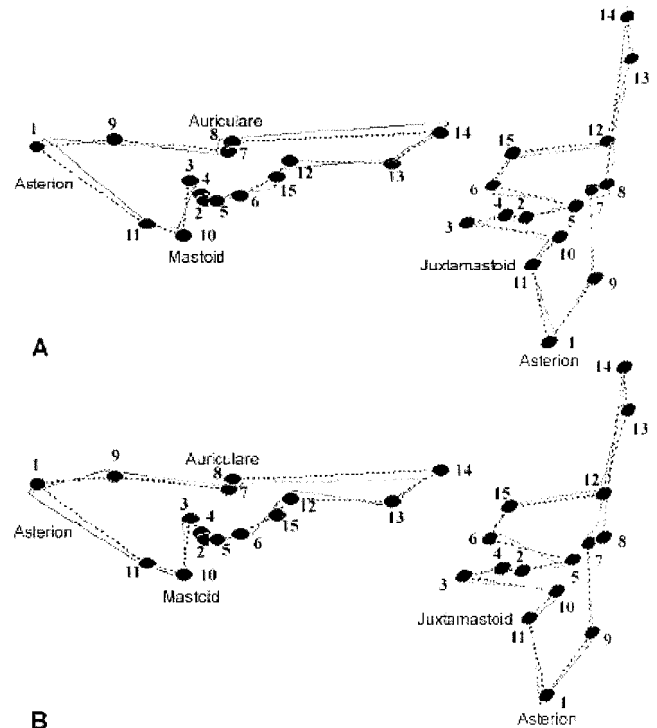


**Fig. 5.** Visualization of shape variation along CVA 3 (step 1) in GRF-ND, right lateral (left) and right ventral (right) views. Displacement vectors show shape differences at each landmark along this axis. Dotted line represents consensus configuration. **A:** Positive (Neanderthal) end. **B:** Negative (modern human) end.

ance and was most strongly influenced by PCs 3, 5, and 10. It was not correlated with centroid size. Neanderthals were significantly different in their mean score value for this canonical axis from all modern human groups. No overlap was observed between Neanderthal and modern human specimens. Amud 1 fell outside of the 95% confidence ellipses of the modern human populations and within the Neanderthal confidence ellipse. Reilingen fell within the Neanderthal 95% confidence ellipse and was far removed from modern human populations. Kabwe, the early anatomically modern human, and the Late Paleolithic European specimens fell well within the range of modern human variation along this axis. The shape differences along CVA 1 included an anterior placement of the lateral origin of the petrotympanic crest and a posterior placement of the medial end of the petrotympanic crest, a superior position of the tip of the mastoid process, a medially placed juxtamastoid eminence, a more laterally and inferiorly placed root of the articular eminence, and a more lateral auriculare and porion (Fig. 6).

CVA 2 (18.8% of total variance, not correlated with centroid size; Fig. 4b) separated Qafzeh 9 from the modern human groups. This specimen fell outside the 95% confidence ellipses of all groups included here, but was closest to the Andamanese. CVA 2 also partially separated the Andamanese and

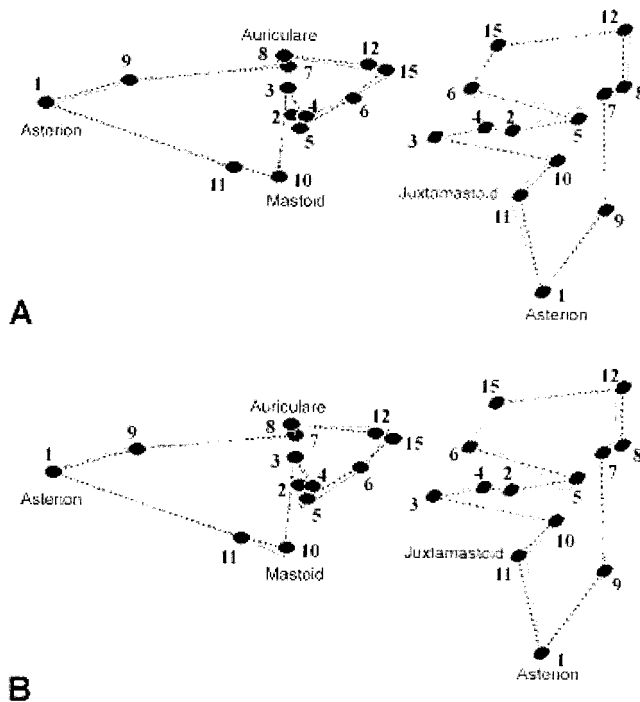


**Fig. 6.** Visualization of shape variation along CVA 1 (step 2) in GRF-ND, right lateral (left) and right ventral (right) views. Displacement vectors show shape differences at each landmark along this axis. Dotted line represents consensus configuration. Landmark numbers correspond to those in Table 3. **A:** Negative (Neanderthal) end. **B:** Positive (modern human) end.

the Khoisan from the other modern human populations, these two groups being significantly different from each other and from most other modern human populations along this axis. Skhul 5 also fell within the 95% confidence ellipse of the Andamanese and outside those of the other modern human groups. Along CVA 2, the anatomically modern human specimens were significantly different from all other populations in their mean scores. The shape differences that characterized Qafzeh 9, and to a lesser extent the Andamanese and Skhul 5, included a laterally placed auriculare, a posteriorly positioned root of the articular eminence, a medially placed medial end of the petrotympanic crest, and an anterior placement of the medial end of the jugular fossa. The opposite shape differences would tend to characterize the Khoisan.

#### Mahalanobis $D^2$ analysis

**Step 1.** The Mahalanobis distances between pairs of groups were calculated (Table 4), taking into account unequal sample sizes (Marcus, 1993). Neanderthals were more distant from the modern human groups than any one modern human population was from another. The group that was closest to Neanderthals was the Inugsuk Eskimo population, although even this distance was so great that it probably does not indicate any particular similarities. Both the two recent European populations and the Late Paleolithic group were very distant from Nean-

derthals. All modern human populations are closest neighbors with their geographic neighbors in this analysis (European, Australo-Melanesian, and sub-Saharan African pairs). The Late Paleolithic specimens were relatively distant from the recent human groups, being closest to the Austrian Berg. These large distances may be overestimated due to the very small sample size of this group (two specimens). Kabwe appeared almost equidistant from modern humans and Neanderthals. Skhul 5 was also very distant from both the modern human groups and Neanderthals, but closer to the former. However, the distances between singletons or extremely small groups and other populations may be overestimated even after taking into account sample size differences, because of the possible extreme misrepresentation of the population that they belong to.

**Step 2.** Results (Table 4) were similar to those obtained in step 1. Neanderthals were very distant from modern humans, the smallest distance between them and any modern human group being greater than the greatest distance between any pair of modern human populations. Neanderthals were again closest to the Inugsuk Eskimo. The recent European populations and the Late Paleolithic group were again found to be very distant from Neanderthals. Among recent human groups, the three geographic pairs still exhibited the smallest distances to their geographic neighbors. The distances between the Late Paleolithic group and the recent human populations were decreased in this step, and were now found to be equivalent to the distances between recent human populations. This reduction could be due either to the inclusion of two additional specimens or to the removal of the two zygomatic suture landmarks. These hypotheses were tested by repeating the analysis on the reduced number of landmarks and on the Late Paleolithic sample included in step 1. The distances between the two Late Paleolithic specimens and recent human populations were again increased, suggesting that the smaller distances observed in step 2 are the result of the increased sample size. The two early anatomically modern humans, Skhul 5 and Qafzeh 9, were included here in one group. They were very distant from both Neanderthals and recent humans, but closer to the latter. Kabwe again showed almost equivalent distances from modern humans and Neanderthals, but closer to the former. Reilingen was found to be very distant from modern humans and closer to Neanderthals, although this distance was also large. As noted above, the distances between singletons or very small groups and the other populations may be overestimated, even after differences in sample size are taken into account.

## DISCUSSION

### Modern humans

The modern human mean temporal bone landmark configuration is characterized by a medio-lat-

erally narrow tympanic area and glenoid fossa, a sagittal orientation of the petrotympanic crest, and a large mastoid process. A strong signal of geographic clustering among modern human groups is present (see also Harvati, 2001a,b, in press), suggesting that the morphology of this region may be under strong genetic control and therefore likely to reflect phylogenetic relationships.

Several traits were found to characterize modern human males relative to females, although there was considerable overlap between the sexes, including a large mastoid process and juxtamastoid eminence, an antero-posteriorly short and supero-inferiorly tall mastoid portion of the temporal bone, and an antero-posteriorly short zygomatic process. The shape differences observed are in agreement with the general principles for sex estimation based on cranial features (e.g., Steele and Bramblett, 1988; White and Folkens, 1991), which indicate a greater overall robusticity and larger mastoid processes in males relative to females. None of the principal components separating males from females are correlated with centroid size, indicating that these differences are not related to differences in centroid size of the temporal bone.

Among modern human populations, the Andamanese population was found to be consistently significantly different from most other modern human groups in the PCA and CVA. This population also consistently showed the largest, or among the largest, Mahalanobis distances from other modern human groups. This is perhaps not surprising, as this sample represents a very small and isolated population. The shape differences that seem to characterize Andamanese temporal bones relative to those of other modern humans include an antero-posteriorly long mastoid portion of the temporal bone, a more superior placement of the zygomatic process and probably also of the glenoid fossa, a more posterior placement of the root of the articular eminence, and a somewhat stronger supramastoid crest.

### Neanderthals

The Neanderthal mean configuration differed from that of modern humans in having a more laterally placed auriculare and porion, a more coronal orientation of the petrotympanic crest, a smaller mastoid process and a more medially placed juxtamastoid eminence, an inferiorly placed entoglenoid pyramid and root of the articular eminence, an antero-posteriorly shorter mastoid portion, and an elevated superior aspect of the zygomatic suture (Fig. 2). The juxtamastoid eminence appeared only slightly larger than that of modern humans, although it was at the same height as, or even lower than, the Neanderthal mastoid process. Neanderthals did not differ significantly from modern humans in their temporal bone centroid size.

Several of these differences were found to separate Neanderthals from modern humans in the statistical analysis. These do not reflect differences in

centroid size, and they include the morphology of the occipito-mastoid area, the tympanic crest, the supra-mastoid crest, the position of the external auditory meatus relative to the zygomatic process and to the glenoid fossa, and the width of the glenoid fossa. The success of the temporal bone traits in separating Neanderthals from modern humans is reflected in the Mahalanobis  $D^2$  analysis, where Neanderthals were found to be much more distant from modern humans than any two modern human populations were from each other. These results are in agreement with previous multivariate analyses of craniofacial measurements (Stringer, 1974, 1989, 1992; Bräuer and Rimbach, 1990; Bräuer, 1992; Turbón et al., 1997), which found Neanderthals to be widely separated from modern humans. However, they disagree with the geometric morphometric study of the differences between Neanderthals and modern humans by Yaroeh (1996), which found the differences between Neanderthals and modern humans to be minimal based on two-dimensional coordinates of cranial landmarks.

**Occipito-mastoid area.** The Neanderthal occipito-mastoid area is described as showing a large juxtamastoid eminence relative to a small mastoid process, traits often considered as derived Neanderthal features (Boule, 1911–1913; Boule and Vallois, 1957; Santa Luca, 1978; Hublin, 1978b; Stringer et al., 1984; Vandermeersch, 1985; Condemi, 1991, 1992; Dean et al., 1998). However, this region is highly variable in modern humans (Taxman, 1963; McKee and Helman, 1991; also personal observations), and considerable confusion exists in the literature over the terminology used to describe it (Hublin, 1978a), while the homology of the structure interpreted as the juxtamastoid eminence in different fossil specimens has been questioned (Schwartz and Tattersall, 1996b). This study follows Hublin (1978a) in his definition of the juxtamastoid eminence as the crest on the medial border of the digastric fossa, which may or may not straddle the occipito-mastoid suture. It is formed by the insertion of the digastric muscle on the lateral side, and can be continuous or to some extent merge with the line formed by the attachment of the superior oblique muscle postero-medially (Hublin, 1978a; McKee and Helman, 1991).

Authors also disagree over the relative contribution of the mastoid process and the juxtamastoid eminence to the subequal height of the two structures in Neanderthals. Trinkaus (1983) found that, when measured from the Frankfurt plane or from the parietal notch, the height of the Neanderthal mastoid process falls within the range of modern humans. Trinkaus (1983) found the great development of the juxtamastoid eminence to contribute more to the appearance of the equal height of the two structures.

Vandermeersch (1981) noted that it is inappropriate to measure the height of the mastoid process

from the Frankfurt horizontal, as the external auditory meatus (one of the points used to define this line) is slightly elevated in Neanderthals relative to modern humans. He followed the Zoja technique in measuring the mastoid process from the deepest point of the digastric fossa, and found Neanderthal mastoids to be much smaller than those of modern humans. Finally, Martínez and Arsuaga (1997) measured the mastoid process from the parietal notch. They found the Neanderthal mastoid process height average to be much lower the modern human mean, and also to fall in the lower parts of the range for Middle Pleistocene specimens and *H. erectus*. These authors proposed that the small mastoid process in Neanderthals is a derived condition.

In this study, the position of the tip of the mastoid was found to be more important in separating Neanderthals from modern humans than the tip of the juxtamastoid eminence in PCA and CVA, suggesting that a reduction in height of this process is actually present in this fossil group. The only specimen with a mastoid process comparable to that found in modern humans is Amud 1. This specimen is less well-separated from modern humans in the temporal bone analysis, probably due to the large size of this structure. The position of the tip of the juxtamastoid eminence was also found to separate modern humans and Neanderthals. This position, however, involved a more medial placement, rather than a larger size, in Neanderthals. This medial position of the juxtamastoid eminence reflects a medio-laterally wide digastric fossa in Neanderthals, also described by Vallois (1969).

**Tympanic area.** The tympanic area in Neanderthals is thought to retain the primitive condition found in *H. erectus*. Neanderthals are described as showing a tympanomastoid fissure, a trait often thought to characterize Asian *H. erectus* (Andrews, 1984; Delson et al., 2001), as the tympanic crest separates their tympanic into an anterior and a posterior area (Vallois, 1969; Trinkaus, 1983; Vandermeersch, 1985; Elyaqine, 1995a; Dean et al., 1998; Minugh-Purvis et al., 2000). This crest is thought to have an anteriorly placed lateral origin in Neanderthals, at the most inferior point of the tympanic tube. In modern humans, on the other hand, this crest is described as having a more posterior lateral origin at the root of the mastoid process, while no tympanomastoid fissure is present. Furthermore, in modern humans, the medial continuation of this crest forms a tall and platelike vaginal plate of the styloid process, and slopes obliquely to its termination at the carotid canal, showing an orientation that approaches the sagittal, rather than the coronal, plane (Schwartz and Tattersall, 1996b; Martínez and Arsuaga, 1997). Neanderthals are thought to show a more coronal orientation of this crest and a supero-inferiorly shorter and less platelike vaginal plate of the styloid process. Some authors, however, consider the orientation of the

petrotympanic crest in these hominids to be sagittal, rather than coronal (Weidenreich, 1943; Stringer, 1984). These traits are generally considered primitive retentions from *H. erectus*, the opposite conditions being derived traits of modern humans (Martínez and Arsuaga, 1997; Schwartz and Tattersall, 1996b; Dean et al., 1998).

This analysis confirmed previous observations of a more anterior placement of the lateral origin of the petrotympanic crest, as well as the more coronal orientation of this crest, in Neanderthals relative to modern humans. The tympanic crest landmarks, and particularly the landmark marking its lateral origin, were very important in separating these two groups in both PCA and CVA and in both steps. A coronal orientation of the tympanic crest was also observed in the Sima de los Huesos Middle Pleistocene fossils by Martínez and Arsuaga (1997), and was observed here in Reilingen, but not in Kabwe (as also found by Martínez and Arsuaga, 1997; see below).

**Supramastoid crest.** The Neanderthal supramastoid crest has been described as variable in expression, but strong relative to that of modern humans (Boule and Vallois, 1957; Vallois, 1969; Heim, 1976; Elyaqine, 1995a). In this analysis, the lateral position of the auriculare in Neanderthals, reflecting a strong supramastoid crest, was found to contribute to the separation of the two groups in both PCA and CVA. This trait is probably a primitive retention. However, it was not found to characterize Kabwe, although a strong supramastoid crest was described for this specimen (Dean et al., 1998; see below).

**Position of external auditory meatus.** An elevated position of the external auditory meatus relative to the zygomatic process and to the floor of the glenoid fossa was previously described for Neanderthals (Vallois, 1969; Vandermeersch, 1985; Hublin, 1988b; Elyaqine, 1995a,b). This feature was more difficult to assess, due to the reduced Neanderthal sample that preserved the zygomatic process. Where the zygomatic suture landmarks were included (step 1), an inferior position of the lateral margin of the glenoid fossa and, to a lesser extent, of the inferior aspect of the zygomatic suture, contributed to the separation of Neanderthals from modern humans in both PCA and CVA. As was also found by Yaroeh (1996), it is the more inferior placement of these structures relative to the porion that results in an apparent elevated position of the external auditory meatus relative to the glenoid fossa and the zygomatic arch in Neanderthals. This shape difference between Neanderthals and modern humans was no longer observed when the two zygomatic suture landmarks were removed.

**Width, depth, and shape of glenoid fossa.** The Neanderthal glenoid fossa is described as wide, shallow, and medially closed off. In this analysis, the

position of the root of the articular eminence, measured at the lateral margin of the glenoid fossa, was found to be more lateral relative to the entoglenoid process in Neanderthals in the CVA of step 2, suggesting a medio-laterally wider glenoid fossa. The depth of the fossa could not be easily assessed, as the analysis did not include a landmark at the deepest point of its floor. However, the root of the articular eminence at the lateral margin of the fossa was found to be more inferiorly placed in Neanderthals in both PCA and CVA of step 1, as well as in CVA of step 2. The inferior position of the lateral margin of the floor of the glenoid fossa may indicate a decreased depth for this structure relative to modern humans. Finally, a more posterior placement of the entoglenoid process was found in the PCA of step 1, in accordance with the description by Vallois (1969) of a medially closed-off glenoid fossa in Neanderthals. This shape difference, however, was not found in the PCA of step 2 or in either CVA, suggesting that it may not be as important as thought by Vallois (1969).

**Western Asian and early Neanderthals.** Neither the Western Asian nor the earlier Neanderthal specimens were treated as separate groups, due to very small sample sizes. However, Amud 1 was the only specimen that consistently overlapped with the modern human range along the axes that separated Neanderthals from modern humans in both PCAs and in the CVA of step 1, although it was clearly separated from it in the CVA of step 2. Although its temporal bone landmark configuration showed a more coronal orientation of the petrotympanic crest and an inferior placement of the root of the articular eminence, it was intermediate between modern humans and Neanderthals in these traits. Furthermore, and perhaps most importantly, it showed a large mastoid process, and in this characteristic it was almost identical to the modern human mean configuration. These traits were noted by Suzuki and Takai (1970), who found the mastoid process of Amud 1 to be of average size for modern humans, as did also Stringer and Trinkaus (1981). Suzuki and Takai (1970) also noted that its glenoid fossa was deeper than that of the European Neanderthals, although shallower than in modern humans, as also observed here, and that the morphology of its tympanic crest fell within the modern human range of variation. The other Western Asian Neanderthal specimen included in this analysis, Shanidar 1, did not show any similarities to Amud 1 or to modern humans in these characteristics, and was always separated from modern humans in PCA and CVA.

The early specimens from Krapina and Saccopastore included here shared the typical temporal landmark configuration that distinguishes Neanderthals from modern humans. The Neanderthal character of the temporal bone of Saccopastore 2 was noted by Condemi (1991, 1992). The Krapina remains were described as possessing a wide range of variation in

temporal, and particularly mastoid, morphology, but still possessing a Neanderthal pattern (Smith, 1982; Minugh-Purvis et al., 2000). The sample in step 2 included only two specimens from Krapina (Krapina C and 39-1), thus not reflecting the entire range of variation in this group, as many of the Krapina temporal bones were too fragmentary to be included. These specimens, however, conformed to the pattern observed in other Neanderthals, and were separated from modern humans in PCA and CVA, confirming previous observations of their essential resemblance to the later Western European Neanderthal sample (Smith, 1982).

**Sexual dimorphism.** Although assignment of sex to fossil specimens is problematic, it is interesting to explore the patterns of dimorphism among the presumed male and female Neanderthal specimens. As all Neanderthal specimens included in step 1 are thought to be male, such a pattern could only be observed in step 2 of the analysis. Neanderthals were found to conform to the relatively weak pattern of sexual dimorphism exhibited by most modern human populations, females showing a smaller mastoid process and an antero-posteriorly elongated and supero-inferiorly short mastoid portion of the temporal bone relative to males.

#### Reilingen

This specimen was only included in step 2. Compared to the mean modern human configuration, it differed in having a smaller mastoid process, a much larger juxtamastoid eminence, a very laterally placed auriculare, and a more coronal orientation of the petrotympanic crest. In all of these features it was similar to Neanderthals. However, compared to the Neanderthal mean configuration, this specimen differed in its somewhat more posterior placement of the lateral origin of the petrotympanic crest, and its relatively larger mastoid process. It differed from both Neanderthals and modern humans in having an antero-posteriorly longer mastoid portion and a more anteriorly placed tip of the mastoid process. This specimen was separated from modern humans and most Neanderthals in the PCA of step 2, reflecting its antero-posteriorly long mastoid portion and anteriorly placed tip of the mastoid. Although Reilingen did not cluster with Neanderthals in the PCA, it was clearly separated from modern humans and fell within the Neanderthal 95% confidence ellipse in the CVA (Fig. 2). The shape differences along this axis included most of the similarities found between the Neanderthal mean configuration and Reilingen. Reilingen was found to be much closer in Mahalanobis  $D^2$  to Neanderthals than to modern humans.

#### Kabwe

This specimen's mean configuration differed from the modern human one in showing a smaller mastoid process, and a medio-laterally wider glenoid fossa. It differed from the Neanderthal mean config-

uration in having a smaller juxtamastoid eminence and a more posterior lateral origin and more sagittal orientation of the petrotympanic crest. It differed from both in its antero-posteriorly short temporal portion of the zygomatic arch, its more posteriorly placed tips of both the mastoid process and the juxtamastoid eminence, and a supero-inferiorly shorter mastoid portion of the temporal bone. Kabwe was separated from modern humans in the PCA of both steps. A posteriorly placed tip of the juxtamastoid eminence, a supero-inferiorly short mastoid portion of the temporal bone, and a small mastoid process were the shape differences that separated this specimen from modern humans. Although Kabwe was described as showing a very strong supramastoid crest (Dean et al., 1998), this trait was not found to separate it from modern humans in this analysis. A weak supramastoid crest has been noted for this specimen (Elyaqtime, 1995a). Kabwe was also found to share with modern humans the more sagittal orientation of the petrotympanic crest, the more posterior position of the lateral origin of this crest, and the absence of a tympanomastoid fissure, as noted previously (Elyaqtime, 1995a; Schwartz and Tattersall, 1996; Martínez and Arsuaga, 1997; Dean et al., 1998). The modern affinities of the temporal bone of this specimen were also discussed by Santa Luca (1978). If the sagittal orientation of the petrotympanic crest and the absence of a tympanomastoid fissure represent derived conditions in modern humans, their presence in Middle Pleistocene African fossil hominids implies a direct relationship between modern humans and the latter fossil group to the exclusion of the European lineage, as previously suggested (Hublin, 1978b; Stringer, 1974, 1989, 1992). In the Mahalanobis  $D^2$  analysis, Kabwe was found to show large distances from both modern humans and Neanderthals, although it was closer to the former, particularly in step 2. This finding is similar to those of Stringer (1974), who found Kabwe to be approximately equally removed from both modern humans and Neanderthals, based on a multivariate analysis of craniofacial measurements, although a somewhat stronger similarity to modern humans was found here for Kabwe's temporal bone.

#### Early anatomically modern human specimens

Skhul 5 was similar to the mean modern human configuration in having a posteriorly placed lateral origin of the petrotympanic crest, a sagittal orientation of this crest, and a large mastoid process which is much larger than its substantial juxtamastoid eminence. It differed from both modern human and Neanderthal mean configurations in showing an antero-posteriorly long mastoid portion of the temporal bone, and a more medially placed entoglenoid pyramid. Skhul 5 was separated from modern humans in the PCA of step 1 along PC 8, where it fell close to the two Late Paleolithic specimens. It was found to be similar to these specimens and different from modern humans in having an inferiorly placed pari-

etal notch and superiorly placed asterion, as well as a more posterior placement of the anterior margin of the jugular fossa and a superior placement of the medial end of the petrotympanic crest. This specimen was found to be distant from both modern humans and Neanderthals in Mahalanobis  $D^2$  in step 1, but closer to the former.

Qafzeh 9 was only included in step 2. Qafzeh 9 was similar to the modern human mean configuration in having a large mastoid process and a very small juxtamastoid eminence. It differed from it in having a medio-laterally wider glenoid fossa, a somewhat more anterior lateral origin of the petrotympanic crest, and a more posteriorly placed root of the articular eminence. Qafzeh 9 differed from both the modern human and the Neanderthal mean configuration in the large medio-lateral distance between the auriculare and porion, indicating a strong and laterally projecting supramastoid crest. Qafzeh 9 was separated from all other human specimens in the CVA. The same axis that separated this specimen from recent humans also separated the Andamanese from the other modern human populations. The shape differences that separated Qafzeh 9 and, to a lesser extent, the Andamanese from other modern humans included a lateral placement of the auriculare and a medial placement of the porion, indicating a strong and laterally projecting supramastoid crest (probably a primitive retention), and a posterior placement of the root of the articular eminence. A prominent supramastoid crest relative to both Skhul 5 and recent humans was also noted for this specimen by Vandermeersch (1981). Qafzeh 9 was considered together with Skhul 5 in the Mahalanobis  $D^2$  analysis. They were found again to show large distances to both modern humans and Neanderthals, but to be closer to the former. These large distances may be due to their very small sample size, but may also partially reflect the distinctive morphology of Qafzeh 9. They are in keeping with the large distances between early anatomically modern human specimens and recent humans previously reported in metric studies of both cranial and postcranial measurements (Stringer, 1974, 1992; Bräuer and Rimbach, 1990; Bräuer, 1992; Kidder et al., 1992; Pearson, 2000), and sometimes interpreted as reflecting retention of pleisiomorphic traits in these specimens (Stringer, 1992).

#### Late Paleolithic specimens

This analysis included two Late Paleolithic specimens in step 1 (Cro Magnon 1 and Predmosti 3) and four in step 2 (additionally Predmosti 4 and Mladec 2). The mean configuration for these specimens was very similar to that of modern humans, exhibiting a large mastoid process, small juxtamastoid eminence, posteriorly placed lateral origin and sagittal orientation of the petrotympanic crest, and an antero-posteriorly long mastoid portion. Among the Late Paleolithic specimens, Mladec 2 showed some similarities to the mean Neanderthal configuration

in having a large juxtamastoid eminence and a relatively strong supramastoid crest, although these traits are combined with a modern human-like posteriorly placed lateral origin and sagittal orientation of the petrotympanic crest. Despite these limited similarities, this specimen never clustered with Neanderthals in either PCA or CVA. The Late Paleolithic specimens as a group were separated from modern humans in the PCA of step 1, reflecting an inferiorly placed parietal notch and superiorly placed asterion, as well as a more posterior placement of the anterior margin of the jugular fossa and a superior placement of the medial end of the petrotympanic crest. These differences were not found in the PCA or the CVA of step 2, where the sample was increased from two to four specimens.

The Mahalanobis distances between this group and recent human populations were relatively large in step 1, but were reduced in step 2, where they appeared equivalent to those found among recent human populations. As discussed above, this difference between the two steps of analysis probably reflects the very small sample size of this group in step 1. These results agree with previous multivariate analyses of craniofacial measurements (Stringer, 1974, 1989, 1992; Bräuer and Rimbach, 1990; Bräuer, 1992; Turbón et al., 1997) that found these specimens to be widely separated from Neanderthals. Kidder et al. (1992) suggested a closer relationship of the Mladec crania to Neanderthals, based on their multivariate analysis of craniofacial measurements. Although limited similarities were found between the mean Neanderthal temporal bone configuration and Mladec 2 (the only specimen from that series included here), these were not found to be important in the statistical analysis.

### CONCLUSIONS

The temporal bone landmarks analysis was very successful in separating Neanderthals from modern humans. Most previously described Neanderthal temporal bone features were supported by this analysis, including the small size of the mastoid process, the orientation of the petrotympanic crest, the anterior position of the lateral origin of the petrotympanic crest, the strong supramastoid crest, and the great width of the glenoid fossa. The apparent elevated position of the external auditory meatus, also previously described as a Neanderthal characteristic, was found here to be due to an inferior placement of the glenoid fossa and zygomatic arch. Finally, the large size of the juxtamastoid eminence in Neanderthals was found to be less important in differentiating this group from modern humans than the small size of the mastoid process.

The temporal bone morphology of several non-Neanderthal fossil specimens was also evaluated in this analysis. Kabwe differed in its temporal bone landmark configuration from both modern humans and Neanderthals, but was found to be slightly closer to modern humans in Mahalanobis distances.

Both distances, however, were quite large. Reilingen was found to be most similar in its landmark configuration and closest in Mahalanobis distance to Neanderthals, although it was intermediate between Neanderthals and modern humans in the size of its mastoid process. The Upper Paleolithic specimens and Skhul 5 exhibited essentially modern human patterns of temporal bone morphology. Qafzeh 9 was characterized by an unusually strong lateral projection of the supramastoid crest. In this trait, this specimen was different from all recent humans, as well as from Skhul 5. Both Qafzeh 9 and Skhul 5 showed large distances to both Neanderthals and modern humans, although they were closer to the latter, probably reflecting the very small sample size for this group but also their distinctive temporal bone morphology.

### ACKNOWLEDGMENTS

I thank the curators and collections managers who kindly allowed me to study the fossil and recent collections in their care: Chris Stringer, Louise Humphrey and Rob Kruszynski, Yoel Rak, George Koufos, Jakov Radovic, Henry de Lumley, Marie-Antoinette de Lumley and Dominique Grimaud-Hervé, Gabriella Spedini and Giorgio Manzi, Roberto Macchiarelli and Luca Bondioli, Patrick Semal and the family of Prof. Max Lohest, Reinhard Ziegler, Maria Teschler, André Langaney and Mario Chech, Horst Seidler and Sylvia Kirchengast, Niels Lynnerup, Wim van Neer, Ross MacPhee, Ian Tattersall, Gary Sawyer, and Ken Mowbray. I am indebted to Bill Howells, Eric Delson, Les Marcus, Michelle Singleton, and David Reddy for their help. I also thank the two anonymous reviewers for their helpful comments and suggestions. This is NYCEP morphometrics contribution no. 8.

### LITERATURE CITED

- Andrews P. 1984. An alternative interpretation of characters used to define *Homo erectus*. *Cour Forsch Seckenberg* 69:167–175.
- Arsuaga JL, Martínez I, Gracia A, Carretero JM, Carbonell E. 1993. Three new human skulls from the Sima de los Huesos Middle Pleistocene site in Sierra de Atapuerca, Spain. *Nature* 362:534–537.
- Boule M. 1911–1913. L'homme fossile de la Chapelle-aux-Saints. *Ann Paleontol* 6:11–172, 7:21–56, 8:1–70.
- Boule M, Vallois HV. 1957. Fossil men. New York: Dryden Press.
- Bräuer G. 1992. Africa's place in the evolution of *Homo sapiens*. In: Bräuer G, Smith F, editors. Continuity or replacement: controversies in *Homo sapiens* evolution. Rotterdam: A.A. Balkema. p 83–98.
- Bräuer G, Rimbach KW. 1990. Late archaic and modern *Homo sapiens* from Europe, Africa and Southwest Asia: craniometric comparisons and phylogenetic implications. *J Hum Evol* 19: 789–807.
- Condemi S. 1991. Circeo I and variability among classic Neanderthals. In: Piperno M, Scichilone G, editors. The Circeo 1 Neanderthal skull: studies and documentation. Rome: Istituto Poligrafico e Zecca dello Stato.
- Condemi S. 1992. Les hommes fossiles de Saccopastore et leurs relations phylogénétiques. *Cahiers de paléanthropologie*. Paris: CNRS Editions.

- Dean D. 1993. The middle Pleistocene *Homo erectus/Homo sapiens* transition: new evidence from space curve statistics. Ph.D. dissertation, City University of New York.
- Dean D, Hublin JJ, Holloway R, Ziegler R. 1998. On the phylogenetic position of the pre-Neanderthal specimen from Reilingen, Germany. *J Hum Evol* 34:485–508.
- Delson E, Harvati K, Reddy D, Marcus LF, Mowbray K, Sawyer GJ, Jacob T, Marquez S. 2001. Sambungmachan 3 *Homo erectus* calvaria: a comparative morphometric and morphological analysis. *Anat Rec* 262:380–297.
- Elyaqnine M. 1995a. Variabilité et évolution de l'os temporal chez *Homo sapiens*. Comparaisons avec *Homo erectus*. Thèse, Université Bordeaux I, no. d'ordre 1321, 215.
- Elyaqnine M. 1995b. Situation du méat auditif par rapport au processus zygomatique chez *Homo erectus* et *Homo sapiens*: implications biomécaniques et phylogénétiques. *C R Acad Sci Ser IIa* 321:347–352.
- Elyaqnine M. 1996. L'os temporal chez *Homo erectus* et *Homo sapiens*: variabilité et évolution. *Rev Archaeom* 20:5–22.
- Genoves S. 1954. The problem of the sex of certain fossil hominids, with special reference to the Neanderthal skeletons from Spy. *J R Anthropol Inst Great Britain Ireland* 84:131–144.
- Harvati K. 2001a. The Neanderthal problem: 3-D geometric morphometric models of cranial shape variation within and among species. Ph.D. dissertation, City University of New York.
- Harvati K. 2001b. Models of shape variation within and among species and the Neanderthal taxonomic position: a 3-D geometric morphometric approach on temporal bone morphology. *J Hum Evol* 40:9–10.
- Harvati K. In press. Models of shape variation between and within species and the Neanderthal taxonomic position: a 3D geometric morphometrics approach. BAR International Series.
- Heim JL. 1976. Les hommes fossiles de la Ferassie. Tome 1, mémoire 35. Archives de l'Institut de Paléontologie Humaine. Paris: Masson.
- Howells WW. 1973. Cranial variation in man: a study by multivariate analysis of patterns of difference among recent human populations. *Pap Peabody Mus* 67. p 1–259.
- Howells WW. 1989. Skull shapes and the map: craniometric analyses in the dispersion of modern *Homo*. *Pap Peabody Mus* 79. p 1–189.
- Hublin JJ. 1978a. Le torus occipital transverse et les structures associées: évolution dans le genre *Homo*. Thèse, Université Pierre et Marie Curie, Paris VI.
- Hublin JJ. 1978b. Quelques caractères apomorphes du crâne néanderthalien et leur interprétation phylogénique. *C R Acad Sci [III]* 287:923–926.
- Hublin JJ. 1988a. Caractères dérivés de la région occipitomastoi-dienne chez les Néandertaliens. *Anat Homme Neandertal* 3:67–73.
- Hublin JJ. 1988b. Les plus anciens représentants de la lignée préneandertalienne. *Anat Homme Neandertal* 3:81–94.
- Jelinek J. 1969. Neanderthal man and *Homo sapiens* in Central and Eastern Europe. *Curr Anthropol* 10:475–503.
- Kidder JH, Jantz RL, Smith FH. 1992. Defining modern humans: a multivariate approach. In: Bräuer G, Smith FH, editors. Continuity or replacement: controversies in *Homo sapiens* evolution. Rotterdam: A.A. Balkema. p 157–177.
- Lahr MM. 1996. The evolution of modern human diversity: a study of cranial variation. Cambridge: Cambridge University Press.
- Marcus LF. 1993. Some aspects of multivariate statistics for morphometrics. In: Marcus LF, Bello E, García-Valdecasas A, editors. Contributions to morphometrics. Madrid: Monograficas Museo Nacional de Ciencias Naturales. p 99–130.
- Martínez I, Arsuaga JL. 1997. The temporal bones from Sima de los Huesos middle Pleistocene site (Sierra de Atapuerca, Spain). A phylogenetic approach. *J Hum Evol* 33:283–318.
- McCown TD, Keith A. 1937. The Stone Age of Mount Carmel, volume II: fossil human remains from the Levallois-Moustérian. Oxford: Clarendon Press.
- McKee JK, Helman SB. 1991. Variability of the hominid juxta-mastoid eminence and associated basicranial features. *J Hum Evol* 21:275–281.
- Minugh-Purvis N, Radovic J, Smith FH. 2000. Krapina 1: a juvenile Neanderthal from the early Late Pleistocene of Croatia. *Am J Phys Anthropol* 111:393–424.
- Oakley KP, Campbell BG, Molleson TI. 1971. Catalogue of fossil hominids, part II: Europe. Kettering: Staples Printers Ltd.
- O'Higgins P, Jones N. 1998. Facial growth in *Cercocebus torquatus*: an application of three-dimensional geometric morphometric techniques to the study of morphological variation. *J Anat* 193:251–272.
- Pearson OM. 2000. Postcranial remains and the origin of modern humans. *Evol Anthropol* 9:229–247.
- Radovic J, Smith FH, Trinkaus E, Wolpoff MH. 1988. The Krapina hominids: an illustrated catalog of skeletal collection. Zagreb: Croatian Natural History Museum.
- Rohlf JF. 1990. Rotational fit (Procrustes) methods. In: Rohlf FJ, Bookstein FL, editors. Proceedings of the Michigan Morphometrics Workshop. Ann Arbor: University of Michigan Museum of Zoology. p 227–236.
- Rohlf JF. 1996. Morphometric spaces, shape components and the effects of linear transformations. In: Marcus LF, Corti M, Loy A, Naylor GJP, Slice DE, editors. Advances in morphometrics. NATO ASI series. New York: Plenum Press. p 117–129.
- Rohlf JF. 1998. TpsSmall, version 1.18. Department of Ecology and Evolution, State University of New York, Stony Brook, New York.
- Rohlf JF. 2000. Statistical power comparisons among alternative morphometric methods. *Am J Phys Anthropol* 111:463–478.
- Rohlf JF, Marcus LF. 1993. A revolution in morphometrics. *Trends Ecol Evol* 8:129–132.
- Santa Luca AP. 1978. A re-examination of presumed Neanderthal-like fossils. *J Hum Evol* 7:619–636.
- Schwartz JH, Tattersall I. 1996a. Significance of some previously unrecognized apomorphies in the nasal region of *Homo neanderthalensis*. *Proc Natl Acad Sci USA* 93:10852–10854.
- Schwartz JH, Tattersall I. 1996b. Toward distinguishing *Homo neanderthalensis* from *Homo sapiens*, and vice versa. *Anthropologie* 34:79–88.
- Slice DE. 1992. GRF-ND: Generalized rotational fitting of n-dimensional landmark data. Department of Ecology and Evolution, State University of New York, Stony Brook, New York.
- Slice DE. 1994–1999. Morpheus et al. Department of Ecology and Evolution, State University of New York, Stony Brook, New York.
- Slice DE. 1996. Three-dimensional generalized resistance fitting and the comparison of least-squares and resistant fit residuals. In: Marcus LF, Corti M, Loy A, Naylor GJP, Slice DE, editors. Advances in morphometrics. NATO ASI series. New York: Plenum Press. p 179–199.
- Slice DE. 2001. Landmark coordinates aligned by Procrustes analysis do not lie in Kendall's shape space. *Syst Biol* 50:141–149.
- Smith FH. 1980. Sexual differences in European Neanderthal crania with special reference to the Krapina remains. *J Hum Evol* 9:359–375.
- Smith FH. 1982. Upper Pleistocene hominid evolution in South-Central Europe: a review of the evidence and analysis of Trends. *Curr Anthropol* 23:667–703.
- Steele GD, Bramblett CA. 1988. The anatomy and biology of the human skeleton. College Station: Texas A&M University Press.
- Stringer CB. 1974. Population relationships of Later Pleistocene hominids: a multivariate study of available crania. *J Archaeol Sci* 1:317–142.
- Stringer CB. 1984. The definition of *Homo erectus* and the existence of the species in Africa and Europe. *Cour Forsch Senckenberg* 69:131–143.
- Stringer CB. 1985. Middle Pleistocene hominid variability and the origin of Late Pleistocene humans. In: Delson E, editor. Ancestors: the hard evidence. New York: Liss. p 289–295.
- Stringer CB. 1989. The origin of early modern humans: a comparison of the European and non-European evidence. In: Stringer C, Mellars P, editors. The human revolution. Princeton: Princeton University Press. p 232–244.
- Stringer CB. 1992. Reconstructing recent human evolution. *Philos Trans R Soc Lond [Biol]* 337:217–224.

- Stringer CB, Trinkaus E. 1981. The Shanidar Neanderthal crania. In: Stringer CB, editor. Aspects of human evolution. London: Taylor and Francis. p 129–165.
- Stringer CB, Hublin JJ, Vandermeersch B. 1984. The origin of anatomically modern humans in Western Europe. In: Smith FH, Spencer F, editors. The origins of modern humans: a world survey of the fossil evidence. New York: Liss. p 51–135.
- Suzuki H, Takai F. 1970. The Amud man and his cave site. Tokyo: Academic Press of Japan.
- Taxman RM. 1963. Incidence and size of the juxtamastoid eminence in modern crania. *Am J Phys Anthropol* 21:153–157.
- Trinkaus E. 1983. The Shanidar Neanderthals. New York: Academic Press.
- Trinkaus E, Smith FH. 1985. The fate of the Neanderthals. In: Delson E, editor. Ancestors: the hard evidence. New York: Liss. p 325–333.
- Turbón D, Pérez-Pérez A, Stringer CB. 1997. A multivariate analysis of Pleistocene hominids: testing hypotheses about European origins. *J Hum Evol* 32:449–468.
- Vallois HV. 1969. Le temporal Néanderthalien H 27 de La Quina. *Étude anthropologique. Anthropologie* 73:524–400.
- Vandermeersch B. 1981. Les hommes fossiles de Qafzeh (Israel). *Cahiers de paléontologie*. Paris: CNRS Editions.
- Vandermeersch B. 1985. The origin of the Neanderthals. In: Delson E, editor. Ancestors: the hard evidence. New York: Liss. p 306–309.
- Weidenreich F. 1943. The skull of *Sinanthropus pekinensis*: a comparative study. *Paleontol Sin New Ser D* 10:1–484.
- White TD, Folkens PA. 1991. Human osteology. San Diego: Academic Press.
- Yaroch LA. 1996. Shape analysis using the thin-plate spline: Neanderthal cranial shape as an example. *Yrbk Phys Anthropol* 39:43–89.